Double Quadriphase Modulation/Demodulation Technique for Three-Channel Communication Link

WADDAH K. ALEM
Axiomatix
Marina del Rey, California

Summary. - A modulation technique for a three-channel communication link is introduced. The structure of the modulator is such as to form an unbalanced quadriphase signal wherein the high rate data stream is bi-phase modulated on the in-phase carrier component, while the sum of the two lower rate signals is bi-phase modulated on the quadrature component of the same carrier. The sum of the two lower signals is, in turn, formed by modulating with the respective data streams the in-phase and the quadrature components of a square wave subcarrier. At the demodulator, the tracking of the carrier and the subcarrier is performed by two independent Costas loops. The demodulation of the high data rate signal is carried out after establishing the carrier reference signal, while the lower rate signals are demodulated after the subcarrier loop recovers the subcarrier. In this paper, the performance of the two loops is analyzed and the expressions for the tracking errors are derived. Finally, a numerical example pertaining to the Space Shuttle-to-TDRS Ku-band link is presented for illustration.

Introduction. - The three-channel modulator forms an unbalanced quadriphase signal wherein the high rate signal $m_1(t)$ is bi-phase modulated on an in-phase carrier. The other two signals, $m_2(t)$ and $m_3(t)$, are quadriphase modulated on a separate subcarrier which is then bi-phase modulated on the quadrature carrier. The two carrier components are then linearly summed, thus forming a composite quadriphase signal. Since the subcarrier modulator output S(t) is a multi-level signal, the composite quadriphase carrier does not have a constant envelope. To provide a constant envelope, the carrier is hard-limited and then power amplified. The ratio of the powers of the various signals can assume any desired value. At the receiver, a Costas loop is used to recover the carrier and a separate Costas loop is then implemented to recover the subcarrier before all three signals can be demodulated.

In this paper, the transmitted signal is defined first and then the tracking performance of both loops is derived. Specifically, expressions for the phase jitter in both loops is found and the effect of cross-talk is considered. A specific numerical example for the case when

This work was supported by the National Aeronautics and Space Administration under Contract No. NAS 9-13467.

the two higher rate signals are NRZ and the lowest rate signal is a Manchester code is carried out for illustration purposes.

Three-Channel Modulator. - The three-channel modulator is shown in Figure 1. The generated signal by the modulator is

$$s(t) = \sqrt{2}\,[C(t)\cos\omega_c t + S(t)\sin\omega_c t]\,, \tag{1}$$

where

$$\begin{aligned} C(t) &= \sqrt{P_2}\,sq_2(t)\,m_2(t) + \sqrt{P_3}\,sq_3(t)\,m_3(t) \\ &= \sqrt{P_2}\,s_2(t) + \sqrt{P_3}\,s_3(t)\,. \end{aligned}$$

The $sq_2(t)$ and $sq_3(t)$ are the two orthogonal subcarrier square waves. Furthermore, it is assumed that all three signals, i.e., $s_1(t)$, $s_2(t)$ and $s_3(t)$ are ± 1 binary waveforms. P_1, P_2 and P_3 are the respective powers of the three channels. After a bandpass hard-limiter, the signal format could be

$$\begin{aligned} s(t) = \sqrt{2}\,\Big\{&\Big[\sqrt{\tilde{P}_1}\,s_1(t) - \sqrt{\tilde{P}_d}\,s_1(t)\,s_2(t)\,s_3(t)\Big]\sin\omega_c t \\ &+ \Big[\sqrt{\tilde{P}_2}\,s_2(t) + \sqrt{\tilde{P}_3}\,s_3(t)\Big]\cos\omega_c t\Big\}, \end{aligned} \tag{3}$$

where

$$\tilde{P}_1 = P_1 C_1^2$$

$$\tilde{P}_2 = [C_1\sqrt{P_2} - C_2\sqrt{P_3}]^2$$

$$\tilde{P}_3 = [C_1\sqrt{P_3} - C_2\sqrt{P_2}]^2$$

$$\tilde{P}_d = P_1 C_2^2$$

$$C_1 = \frac{1}{2}\left[\frac{1}{\sqrt{1 + 2\sqrt{P_2/P_T}\,\sqrt{P_3/P_T}}} + \frac{1}{\sqrt{1 - 2\sqrt{P_2/P_T}\,\sqrt{P_3/P_T}}}\right]$$

$$C_2 = \frac{1}{2}\left[\frac{1}{\sqrt{1 - 2\sqrt{P_2/P_T}\,\sqrt{P_3/P_T}}} - \frac{1}{\sqrt{1 + 2\sqrt{P_2/P_T}\,\sqrt{P_3/P_T}}}\right] \tag{4}$$

and P_T is the sum of powers in the three channels, namely, $P_T = P_1 + P_2 + P_3$. It can be seen that the signal powers due to hard-limiting are redistributed and a triple cross-product term

is generated. The physical significance of this term has been described in [2].

Carrier Tracking Loop. - At the receiver, the carrier is recovered via a Costas loop, as shown in Figure 2. The received signal can be written as

$$x(t) = s[t,\theta(t)] + n(t) , \tag{5}$$

where

$$s[t,\theta(t)] = \sqrt{2}\left[\sqrt{\tilde{P}_1}\, s_1(t) - \sqrt{\tilde{P}_d}\, s_1(t)\, s_2(t)\, s_3(t)\right] \sin\left[\omega_c t + \theta(t)\right]$$
$$+ \sqrt{2}\left[\sqrt{\tilde{P}_2}\, s_2(t) + \sqrt{\tilde{P}_3}\, s_3(t)\right] \cos\left[\omega_c t + \theta(t)\right] + n(t) . \tag{6}$$

In (6) ω_c is the carrier frequency, $\theta(t)$ is a random phase to be estimated, and n(t) is a narrowband additive white Gaussian noise-given by

$$n(t) = \sqrt{2}\left[N_c(t) \cos\left(\omega_c t + \theta(t)\right) - N_s(t) \sin\left(\omega_c t + \theta(t)\right)\right] , \tag{7}$$

where $N_c(t)$ and $N_s(t)$ are approximately statistically independent, stationary white Gaussian noise processes with single-sided noise spectral density N_0 (watts/Hz).

The Costas loop multiplies the in-phase and quadrature-phase signals by the reference signals

$$r_s(t) = \sqrt{2}\, K_1 \sin \hat{\phi}(t)$$
$$r_c(t) = \sqrt{2}\, K_1 \cos \hat{\phi}(t) , \tag{8}$$

respectively. In (8), $\hat{\phi}(t)$ represents the estimate ($\phi(t) = \omega_c t + \theta(t)$).

Assuming that $S_i(f)$ is the power spectral density of $s_i(t)$; i= 1,2,3, $|G(j\,2\pi f)|^2$ is the square magnitude of the arm filter transfer function, and $S_d(f)= S_1(f)*S_2(f)*S_3(f)$, where the asterisk denotes convolution. Then after considerable manipulation [1], the equivalent loop signal-to-noise ratio ρ'

$$\rho' = \frac{\left(\tilde{P}_1 D_1 - \tilde{P}_2 D_2 - \tilde{P}_3 D_3 + \tilde{P}_d D_d\right)^2}{N_{eq} B_L} \triangleq \rho S_L , \tag{9}$$

where $\rho = P_T/N_0B_L$ is the loop signal-to-noise ratio of a phase-locked loop operating on total power P_T, B_L is the single-sided loop noise bandwidth, D_i and D_d are given by

$$D_i \triangleq \int_{-\infty}^{\infty} S_i(f)\,|G(j\,2\pi f)|^2\,df \qquad i = 1,2,3$$

$$D_d \triangleq \int_{-\infty}^{\infty} S_d(f)\,|G(j\,2\pi f)|^2\,df\,, \tag{10}$$

and N_{eq} is the equivalent noise power given by

$$N_{sq} = 4N_0\left\{\sum_{i=1}^{3}\tilde{P}_i\int_{-\infty}^{\infty}S_i\,|G(j\,2\pi f)|^2\,df + \tilde{P}_d\int_{-\infty}^{\infty}S_{\hat{d}}(f)\,|G(j\,2\pi f)|^2\,df\right\}$$

$$\times\left[1 + \frac{2\int_{-\infty}^{\infty}\frac{N_0}{2}\,|G(j\,2\pi f)|^2\,df}{N_0\left[\sum_{i=1}^{3}P_i\int_{-\infty}^{\infty}S_i(f)\,|G(j\,2\pi f)|^4\,df + \int_{-\infty}^{\infty}S_{\hat{d}}(f)\,|G(j\,2\pi f)|^2\,df\right]}\right]. \tag{11}$$

$S_{\hat{d}}(f)$ is given by

$$S_{\hat{d}}(f) \triangleq S_1(f)\,|G(j\,2\pi f)|^2 * S_2(f)\,|G(j\,2\pi f)|^2 * S_3(f)\,|G(j\,2\pi f)|^2\,. \tag{12}$$

In (9), S_L represents the loop squaring loss which, after much simplification, could be expressed as

$$S_L = \frac{(\eta_1 D_1 - \eta_2 D_2 - \eta_3 D_3 + \eta_d D_d)^2}{\bar{D}\left(\bar{K}_D + \frac{K_L}{\rho_i\bar{D}}\right)} \tag{13}$$

where

$$\eta_i \triangleq \frac{\tilde{P}_i}{P_T}\,; \qquad i = 1,2,3$$

$$\eta_d \triangleq \frac{\tilde{P}_d}{P_T}$$

$$\bar{D} \triangleq \eta_1 D_1 + \eta_2 D_2 + \eta_3 D_3 + \eta_d D_d$$

$$K_L = \frac{\int_{-\infty}^{\infty} |G(j\,2\pi\,f)|^4\,df}{\int_{-\infty}^{\infty} |G(j\,2\pi\,f)|^2\,df}$$

$$B_i = \int_{-\infty}^{\infty} |G(j\,2\pi\,f)|^2\,df$$

$$\bar{K}_D = \frac{\sum_{i=1}^{3} \eta_i \int_{-\infty}^{\infty} S_i(f)\,|G(j\,2\pi\,f)|^4\,df + \eta_d \int_{-\infty}^{\infty} S_{\hat{d}}(f)\,|G(j\,2\pi\,f)|^2\,df}{\sum_{i=1}^{3} \eta_i \int_{-\infty}^{\infty} S_i(f)\,|G(j\,2\pi\,f)|^2\,df + \eta_d \int_{-\infty}^{\infty} S_d(f)\,|G(j\,2\pi\,f)|^2\,df} \quad (14)$$

and $\rho_i = 2\,P_T/N_0\,B_i$ is the total power-to-noise ratio in the arm filter noise bandwidth B_i which is defined as two-sided.

In the linear region of operation [3], the variance of the carrier loop phase error is given by

$$\sigma_{2\varphi}^2 = \frac{1}{\rho'} \cdot \quad (15)$$

Subcarrier Tracking Loop. - The input to the subcarrier tracking loop is taken from the output of the quadrature detector of the carrier tracking loop, as shown in Figure 2. The subcarrier tracking loop is illustrated in Figure 3. Its input $x_{sc}(t)$ is given by

$$x_{sc}(t) = \left[\sqrt{2\tilde{P}_2}\,s_2(t) + \sqrt{2\tilde{P}_3}\,s_3(t) + N_c(t)\right]\cos\varphi_c(t) + \left[\sqrt{2\tilde{P}_1}\,s_1(t) - \sqrt{2\tilde{P}_d}\,s_1(t)\,s_2(t)\,s_3(t) - N_s(t)\right]\sin\varphi_c(t)\,, \quad (16)$$

where $\varphi_c(t)$ = carrier tracking loop phase error.

As is shown in Figure 3, the composite subcarrier signal is bandpass filtered by H(s). The bandwidth of the filter is such that only the fundamental component of the subcarrier is applied to the subcarrier Costas loop.

Letting $H_\ell(j\omega)$ be the lowpass equivalent of $H(j\omega)$ and denoting the cascade filter by

$$G_0(s) \triangleq H_\ell(s)\,G(s)\,, \quad (17)$$

the equivalent loop signal-to-noise ratio in the subcarrier Costas loop is found to be [4]

$$\rho'_{sc} = \frac{\rho_{sc}}{4} S_{L_{sc}}, \tag{18}$$

where $\rho_{sc} = P_T/N_0B_L$ is the loop signal-to-noise ratio with a total power P_T and $S_{L_{sc}}$ is the squaring loss given by

$$S_{L_{sc}} = \frac{\left\{\cos \varphi_c \left(\frac{4}{\pi}\right)^2 [\tilde{P}_2 D_2 - \tilde{P}_3 D_3]\right\}^2}{\widehat{\eta D K}_D + \frac{K_L B_i/R_2}{2 PT_2/N_0} + 2\left(\frac{4}{\pi}\right)^4 \eta_2 \eta_3 \left(\frac{PT_2}{N_0}\right)\frac{D_{23}}{T_2}}, \tag{19}$$

where

$$R_2 = \frac{1}{T_2} \text{ is the higher data rate in the subcarrier loop}$$

$$D_{23} \triangleq \frac{1}{2\pi} \int_{-\infty}^{\infty} S_2(\omega)\, S_3(\omega)\, |G_0(j\omega)|^2\, d\omega$$

$$\widehat{\eta D K} \triangleq \left(\frac{4}{\pi}\right)^2 \left[\sum_{i=2}^{3} \eta_i \int_{-\infty}^{\infty} S_i(\omega)\, |G_0(j\omega)|^2\, \frac{d\omega}{2\pi} + \int_{-\infty}^{\infty} \left(\eta_1 S_1(\omega) + \eta_d S_d(\omega)\right) |G_0(j(\omega - \omega_{sc}))|^2\, \frac{d\omega}{2\pi}\right]; \tag{20}$$

B_i, K_L and η_i are obtained from (14) by substituting $G_0(s)$ for $G(s)$, and D_i is obtained from (10) in a similar manner.

In the derivation of (19), it is arbitrarily assumed that $R_2 > R_3$. This, however, need not be the case because there is no apparent restriction on the relation between R_2 and R_3.

The tracking phase jitter performance in the linear region can be represented as the variance of the subcarrier loop phase error ($2\varphi_{sc}$)

$$\sigma^2_{2\varphi_{sc}} = \frac{1}{\rho'_{sc}} = \frac{4}{\rho_{sc} S_{L_{sc}}}, \tag{21}$$

where ρ'_{sc} is given in (18). However, since the demodulation reference signals are at ω_{sc}, rather than $2\omega_{sc}$, then the jitter on the output of the data streams is

$$\sigma^2_{\varphi_{sc}} = \frac{1}{4}\sigma^2_{2\varphi_{sc}} = \frac{1}{\rho_{sc} S_{L_{sc}}} . \quad (22)$$

Numerical Example. - The Ku-band return link of the Shuttle Orbiter to TDRS is taken as an example. The typical data rates and the signal formats of this link are shown in Table 1.

Table 1. Typical Shuttle-to-TDRS Ku-Band Link Signal Formats

Signal	Rate	Format
$m_1(t)$	10- 100 Mbps	NRZ
$m_2(t)$	200 kbps- 2 Mbps	NRZ or Manchester
$m_3(t)$	192 Mbps	Manchester

The ratio of signal powers P_1, P_2 and P_3 to the total power (P_T) is taken in this example as 0.8, 0.16 and 0.04 , respectively. The restriction on the ratio of powers in each loop is discussed in [5], where it is shown that the conventional Costas loop fails to track only when the ratio of power between the two quadriphase components is unity. It is thus believed that the ability of the three-channel receiver to function is not restricted by the power division as long as the ratio of powers is sufficiently below unity.

The numerical evaluation of the subcarrier tracking jitter (22) is shown in Figures 4 and 5 for the case when $m_1(t)$ and $m_2(t)$ are NRZ while $m_3(t)$ is a Manchester code. The jitter includes the effect of both thermal noise and channel interaction. Several assumptions are made in performing the calculations:

(1) The carrier tracking loop is tracking perfectly; thus, $\cos \varphi_c = 1$.
(2) The bandwidth, H(s), of the bandpass filter is much wider than that of the lowpass arm filters, G(s), in the subcarrier loop.
(3) The arm filters in the subcarrier loop are assumed to be one-pole Butterworth (RC) filters.

Figure 4 indicates that, for a given signal-to-noise ratio of $P_T T_2/N_0$, the subcarrier error decreases with B_i/R_2 ratio. This information is useful for selecting the proper design values for B_i given the value of R_2 and P_T/N_0, which is generally recognized as the link C/N_0.

Figure 5 shows that, for a given set of B_i/R_2 and $P_T T_2/N_0$ ratios, the subcarrier tracking error degrades only slightly with a significant increase in the Channel 2 rate R_2.
Conclusion. - A modulation and a corresponding demodulation technique for a three-channel communication link has been presented. Two independent conventional Costas

loops are used at the receiver to recover the quadriphase modulated carrier and subcarrier. Analytical expressions of the phase jitter were derived for the carrier and subcarrier loops. Typical parameters pertaining to the Ku-band return link of the Shuttle Orbiter were presented for illustration.

References

1. G. K. Huth. “Integrated Source and Channel Encoded Digital Communication System Design Study,” Final Report. Axiomatix Report No. R7607-3, July 31, 1976.

2. B. H. Batson, G. K. Huth, and S. Udalov. “Phase Multiplexing for Three-Channel Data Transmission.” NTC Proceedings, Vol. II, November/ December 1976, Dallas, Texas.

3. W. C. Lindsey and M. K. Simon. Telecommunication System Engineering. Englewood Cliffs, N.J.: Prentice-Hall, Inc., 1973.

4. M. K. Simon. “Subcarrier Tracking Analysis for Three-Channel Orbiter Ku-Band Return Link.” Axiomatix Report No. R7707-4 (under Contract No. NAS 9-15240), July 28, 1977.

5. C. L. Weber. “Candidate Receivers for Unbalanced QPSK.” ITC, September 1976, Los Angeles, California.

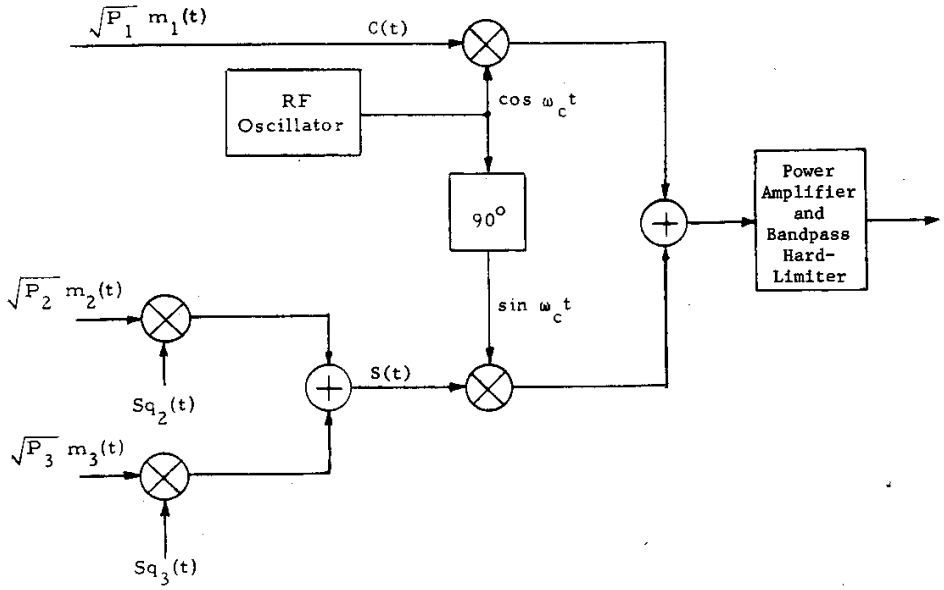

Fig.- 1. Three-Channel Quadrature Multiplex Modulator

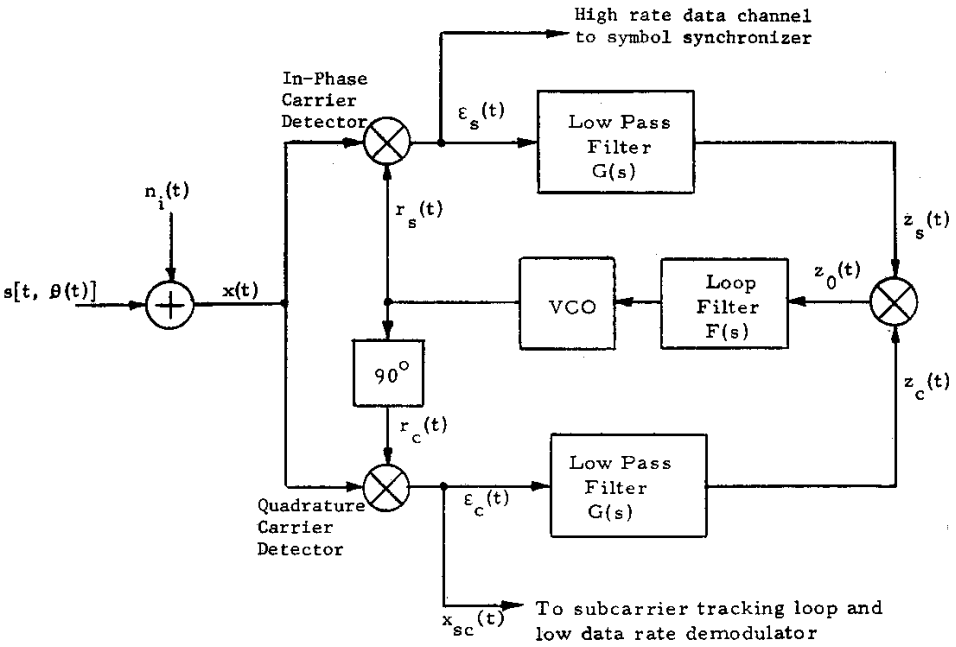

Figure 2. Costas Loop for Carrier Tracking.

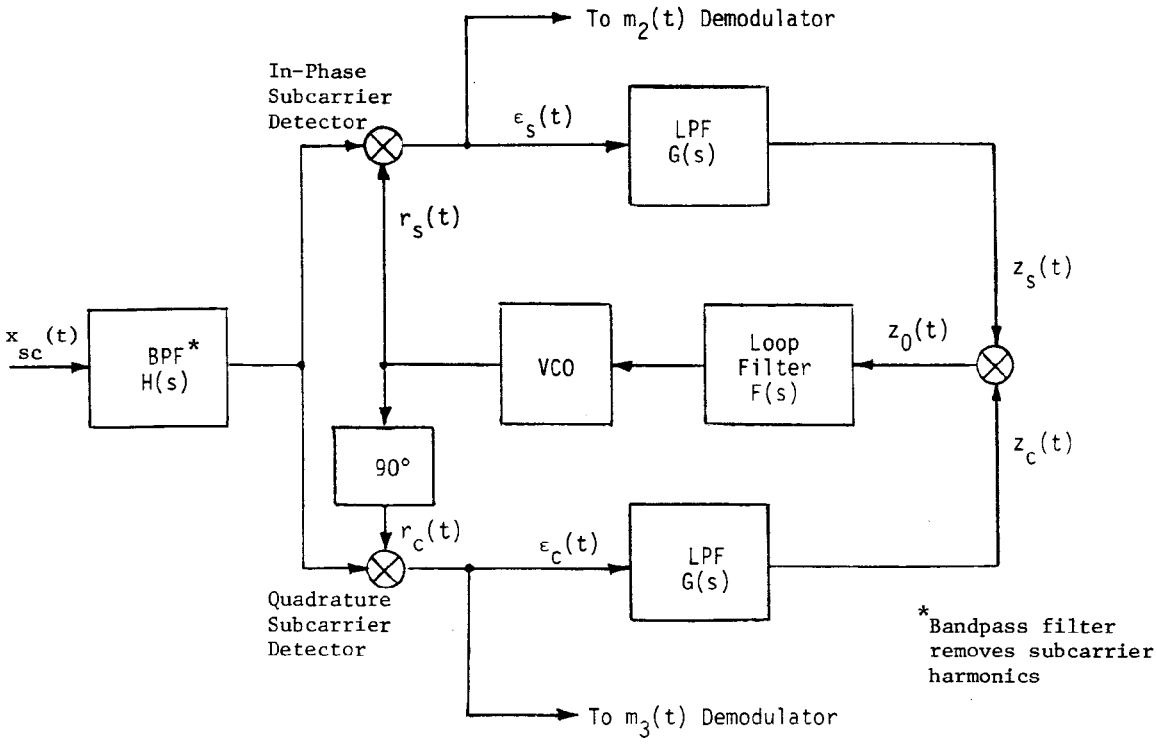

Figure 3. Costas Loop for Subcarrier Tracking

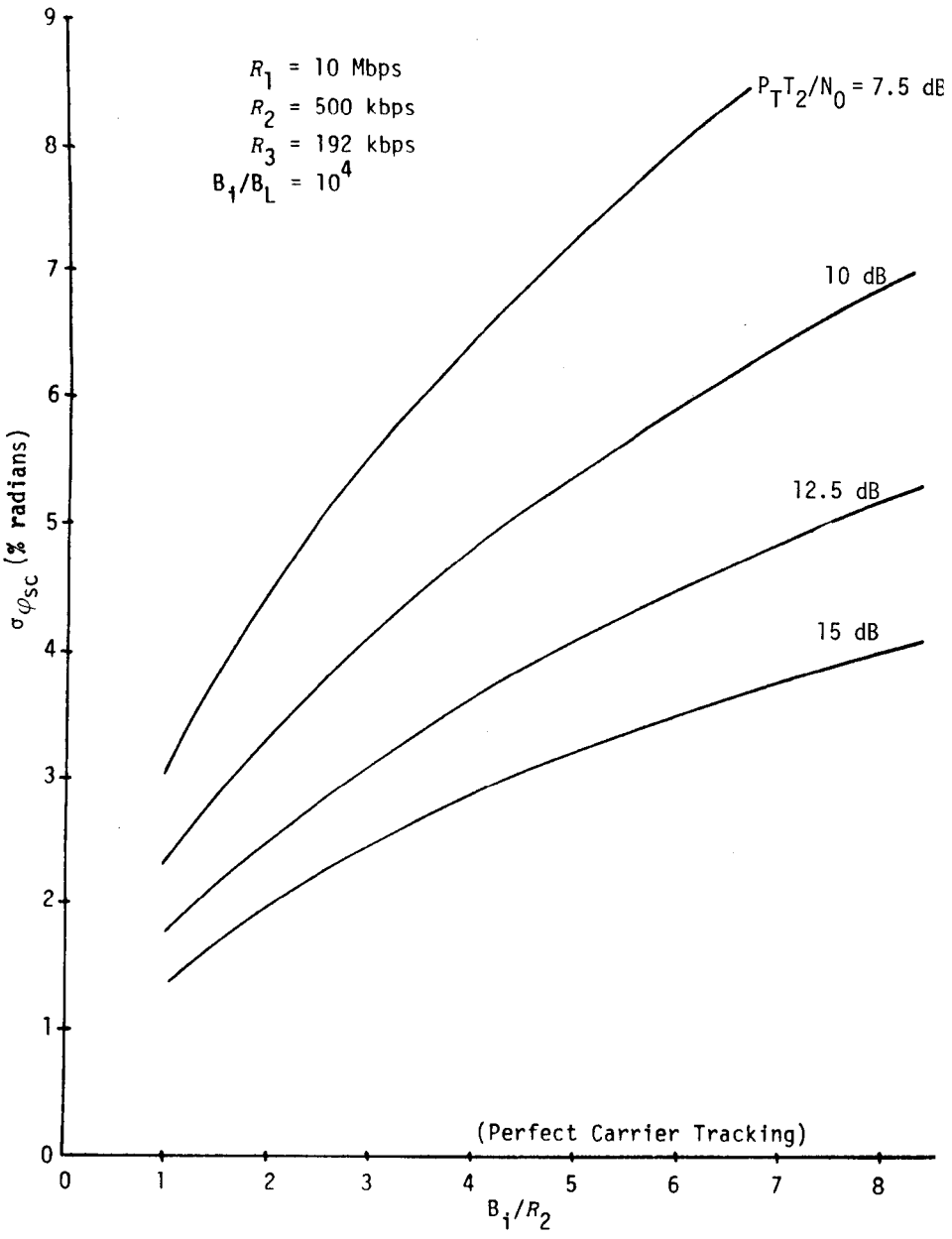

Figure 4. Subcarrier Tracking Jitter versus Ratio of Arm Filter Bandwidth to High Subcarrier Data Rate R_2; P_TT_2/N_0 is a parameter; $m_1(t)$ and $m_2(t)$ are NRZ, $m_3(t)$ is Manchester; $R_1 > R_2 > R_3$.

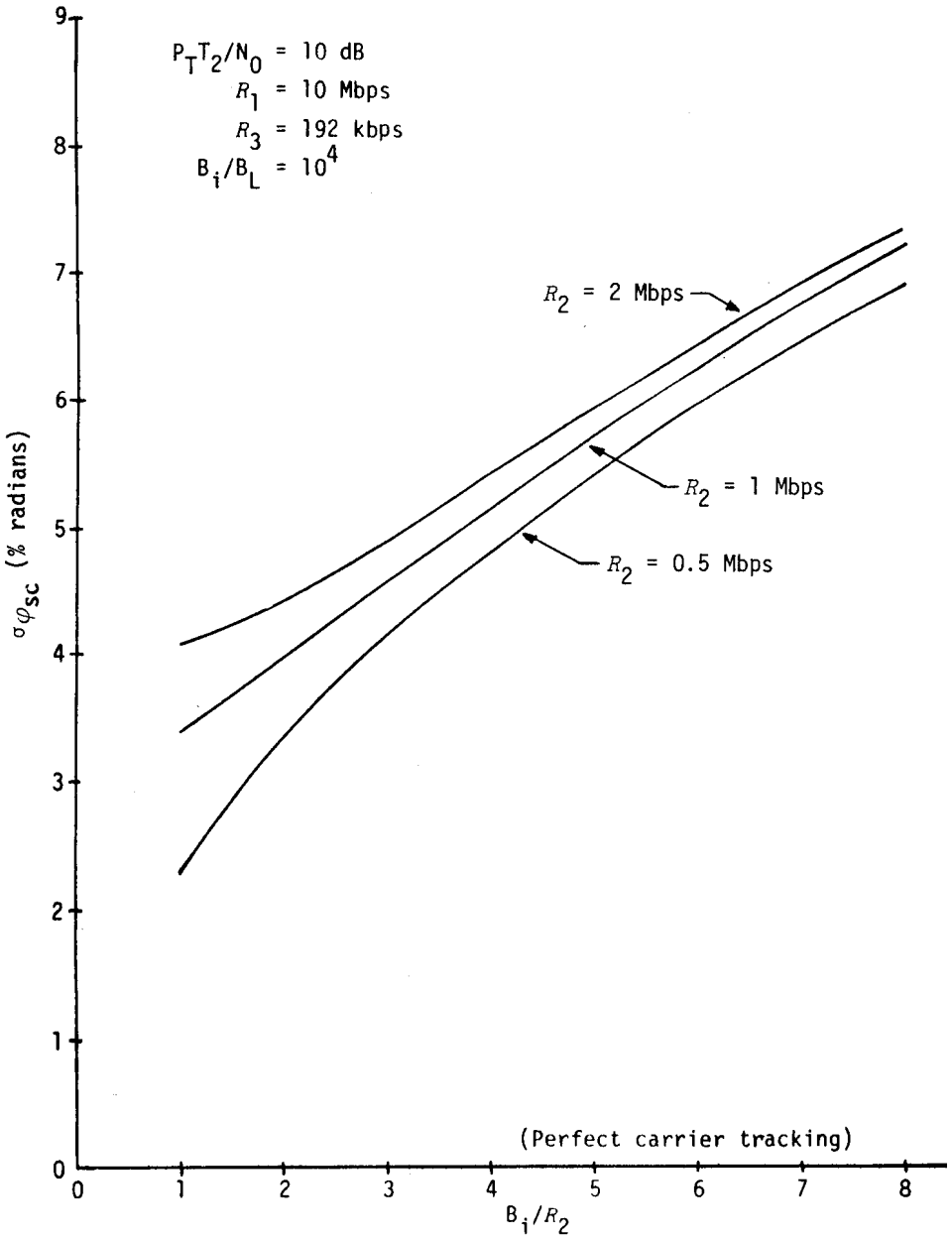

Figure 5. Subcarrier Tracking Jitter versus Ratio of Arm Filter Bandwidth to High Subcarrier Data Rate R_2; R_2 is a parameter; $m_1(t)$ and $m_2(t)$ are NRZ, $m_3(t)$ is Manchester code; $R_1 > R_2 > R_3$.